Towards a Wind Tunnel Testing Environment for Rotorcraft Operations Close to Obstacles

Neda Taymourtash
PhD Candidate
Politecnico di Milano
University of Glasgow
Milan, Italy

Daniele Zagaglia
Post-Doc Research Fellow
Politecnico di Milano
Milan, Italy

Alex Zanotti
Assistant Professor
Politecnico di Milano
Milan, Italy

Giuseppe Gibertini
Associate Professor
Politecnico di Milano
Milan, Italy

Giuseppe Quaranta
Associate Professor
Politecnico di Milano
Milan, Italy

ABSTRACT

The correct identification of the aerodynamic loads due to interaction between rotorcraft and obstacles requires to run computationally intensive numerical models characterized by a high level of uncertainty. Wind tunnel data can be used as a source of information to improve those models. The present paper investigates the aerodynamic interaction of a helicopter and ship airwake exploiting wind tunnel data. A series of wind tunnel experiment, using a scaled helicopter model and Simple Frigate Shape 1, has been performed to measure forces and moments acting on the rotor, while the helicopter is approaching the flight deck. In addition, the velocity components along the longitudinal symmetry plane of the rotor have been visualized using PIV technique. With the rotor positioned at the starting point of the landing trajectory, the load measurements are used to modify the distribution of the inflow over the rotor in multibody simulation environment, in order to generate same loads, including thrust, torque and in-plane moments. Then, an identification algorithm is developed to capture the effect of ship airwake on the rotor loads during the maneuvers, modeling it as an external gust to the rotor inflow. The gust velocity is obtained through an optimization algorithm with the objective of generating same load coefficients as the experiment. The simulation results show that the same load coefficients as the experiment can be generated by implementing a linear gust over the rotor with a magnitude that changes as the rotor moves through the wake of ship. The experiment showed that this test setup could be used for identification of aerodynamic interaction to be used for maneuver analysis.

NOTATION

*

c	Blade chord (m)
C_h	Hub moment coefficient($\sqrt{C_m^2 + C_l^2}$)
C_m, C_l, C_q	Moment coefficients ($M_y/\rho A_r R V_{TIP}^2$)
C_t	Thrust coefficient ($T/\rho A_r V_{TIP}^2$)
f_x, f_y	Empirical factor for longitudinal and lateral inflow distribution
M_{TIP}	Mach number at blade tip
M_x, M_y	Rotor roll and pitch moments (N.m)
R	Rotor radius (m)
Re_{TIP}	Reynolds number at blade tip
T, Q	Rotor thrust and torque (N, N.m)
V_∞	Free stream velocity (m/s)
v_i	Induced velocity (m/s)
X_r, Y_r, Z_r	Rotor reference frame
V_g	Gust velocity (m/s)
χ	Skew angle of the wake
$\lambda_0, \lambda_s, \lambda_c$	Inflow variables
μ	Advance ratio
Ω	Angular velocity of the rotor
ψ	Azimuth angle

INTRODUCTION

Helicopters are regularly required to perform challenging missions in confined areas and close to obstacles. Search and rescue missions over land and water, urban transport, intervention in natural disasters such as flooding or earthquake are some examples in which rotorcraft interacts with the surrounding environment. In these situations, performance and handling qualities of the rotorcraft are highly affected by the presence of the obstacles in close proximity. Offshore operations, like those involving rotorcraft, from and to moving decks and ships are among the most demanding tasks for pilots. In this case, due to the combination of moving flight deck, flying close to the ship hangar wall, changing speed and direction of the wind and turbulent ship airwake, pilot workload is significantly increased which may endanger the safety of flight. It has been shown that the most of the frequency content of the unsteady airwake is concentrated in the range of 0.2-2 Hz (Ref. 1). This bandwidth covers the widely accepted range of pilot closed-loop control frequencies which is less than 1.6 Hz.

The complex aerodynamic environment under which such operations take place is expected to affect directly the handling qualities, and so pilot workload and safety of operation. Analysis of safety operating limits for such demanding missions needs a series of flight test which are inherently hazardous and extremely expensive. Currently, those assessments are typically done only for the most demanding operations such as those of military helicopters operating on moving ships. Each combination of ship-rotorcraft should be tested for a range of wind speed and direction in order to find a safe flight envelope. Consequently, development of the helicopter-obstacle Dynamic Interface Simulation (DIS) is considered as a viable solution which reduces the cost and hazards of time-consuming at-sea test campaigns (Ref. 2). Such a simulation tool could be used to find the optimal trajectory for safe landing and to design and test of new flight control systems. A better understanding of the environmental conditions could lead to the development of more accurate simulation environment for such demanding operation to improve pilot training. All those elements will contribute to the improvement of safety of rotorcraft operations, which is the objective of the NITROS project (Ref. 3).

Regarding the complexity of the flow field generated by the rotorcraft-ship interaction, development of an appropriate airwake model which can capture the induced airloads of the rotor is of great importance. Various numerical or experimental approaches can be taken for airwake modeling which result in different levels of the simulation fidelity. The effect of coupling is worth to be considered in both numerical and experimental analysis of the shipboard operation. The most simplified approach is uncoupled simulation which means there is no interaction between rotorcraft and ship airwake. One-way coupling approach, which has been extensively implemented in simulation environments so far, accounts only for the effect of ship airwake on the rotor inflow. In this approach, the unsteady ship airwake data is pre-calculated using Computational Fluid Dynamics (CFD) and stored in the form of look-up tables (Ref. 4). However, since the airwakes and rotor dynamics are unsteady and nonlinear, the correctness of the overall solution obtained by the principle of superposition is highly questionable. The validity of this assumption has been investigated and proven to be inaccurate in the case of close proximity between two bodies (Ref. 5).

The more promising approach is two-way coupling or fully coupled simulation which includes mutual effect of the rotorcraft and ship airwake. In this approach, the CFD solver and flight dynamics simulation are run simultaneously with communication between two codes. The flight dynamics code calculates the loading of the rotor, as well as the attitude and position of the rotorcraft, which are passed to the CFD code. Then, the local velocity data is computed by CFD solver and fed back to the flight dynamics simulation (Refs. 6–8). Depending on the computational cost of the numerical algorithm, this approach might be used in real time flight simulation. However, the results of coupled simulation needs to be validated with experimental tests.

The approach taken in this research relies on wind tunnel experiments in order to improve the fidelity of flight dynamics simulation. This is the first step towards development of a fully coupled flight dynamics simulation with wind tunnel in the loop.

It is notable that different measurements can be used to communicate the information about the flow field from the experiment to the full scale flight simulator. Assuming that all requirements of dynamic similarity has been satisfied in the experiment, it would be possible to scale up the measured loads and transfer them directly to the full scale flight simulator. However, from practical point of view this is not a feasible solution, since the tip Mach number and Reynolds number of the full scale model cannot be replicated in the experiment, and a full dynamic scaling of the helicopter model is unfeasible without driving the size of obstacles to an unacceptable size. Therefore, the load measurements cannot be transferred directly to the full scale flight simulator.

To better understand the variables of the rotor response, a second-order quasi-steady approximations of the rotor dynamics can be considered:

$$D_2\ddot{\vec{q}} + D_1\dot{\vec{q}} + D_0\vec{q} = D_g\vec{u}_g + D_c\vec{u}_c \qquad (1)$$

Here, $\vec{q}$ consists of all rotor states (including rigid and elastic states) and inflow variables. To incorporate the inflow variables into this model, the theory of dynamic inflow should be implemented which relates the airloads of the rotor to the induced-flow distribution over the rotor disk. The classical model of the dynamic inflow is that of Pitt-Peters with three inflow states, consisting of uniform and linear perturbations of the wake-induced downwash at the rotor disk, which is presented by the following set of first-order differential equations (Ref. 9):

$$[M] \begin{Bmatrix} \dot{\lambda}_0 \\ \dot{\lambda}_s \\ \dot{\lambda}_c \end{Bmatrix} + [L]^{-1} \begin{Bmatrix} \lambda_0 \\ \lambda_s \\ \lambda_c \end{Bmatrix} = \begin{Bmatrix} C_t \\ C_l \\ C_m \end{Bmatrix} \qquad (2)$$

In a higher-order dynamic wake model, the induced-flow distribution can be represented in terms of harmonic variations (Fourier series) in azimuth and arbitrary radial distribution functions, so that it provides a complete description of the unsteady wake induced-flow (Refs. 10, 11). However, the low-frequency model of Pitt-Peters is generally sufficient to capture the wake effects on the dynamic behavior of the lowest-frequency blade modes and the aircraft flight dynamics (Ref. 12). In Ref. 13, the state-space inflow model was identified by applying a numerical identification technique using the inflow response data from viscous Vortex Particle Method (VPM) simulation.

Equation 1 clearly shows that the rotor loads are not only function of rotor states and inflow variables, but also affected by gust velocities. Consequently, it can be expected to reproduce the low-frequency contents of the rotor response (in terms of loads) by taking these two steps:

- reconstructing the average and linear variation of the inflow

- identifying a gust model that is representative of the unsteady wake caused by interaction with surrounding environments

Another solution can be proposed to capture both induced flow and gust effects based on full survey of the flow field around the rotor using a dynamic time resolved PIV (Particle Image Velocimetry) setup. However, implementation of the PIV setup while doing a dynamic test in which rotorcraft is approaching the flight deck is extremely challenging. Consequently, it is proposed to develop an identification algorithm to use the measured loads of a scaled rotorcraft operating close to an obstacle to identify the inflow variables and gust velocities. This parameters are implemented in the full scale model to have a more realistic simulation environment. Figure 1 shows a block diagram of the approach proposed in this research. The identification algorithm developed in this study will be used in the closed-loop communication between flight simulator and wind tunnel in the future experiments.
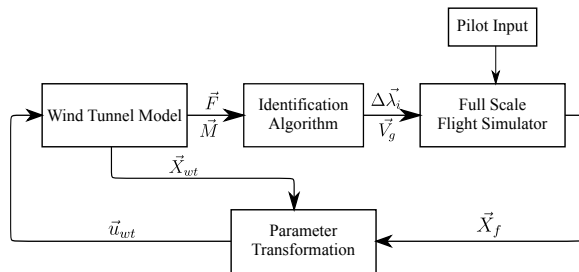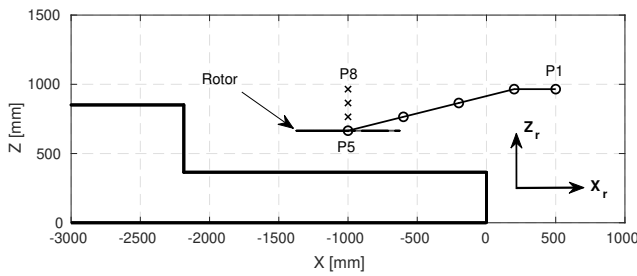
EXPERIMENTAL SETUP AND TEST POINTS

Considering the shipboard operation as one of the most interactive missions which results in a complex flowfield that increases substantially the workload of the pilot, the experiment was designed to simulate a landing trajectory of a scaled helicopter on a generic ship. Since the details of the ship superstructure have not been considered interesting in this research, the Simple Frigate Shape 1 has been selected which is a highly simplified but representative ship geometry, developed as a part of an international collaboration in which Canada, Australia, UK and USA evaluated the ability of CFD codes to simulate complex airwakes (Ref. 14). This model has been scaled down with a geometric factor of 12.5 in order to have enough space on the flight deck for landing of the helicopter model. The experiments were conducted in the environmental test chamber of the Large wind tunnel of Politecnico di Milano (GVPM, see (Ref. 15)). Taking advantage of the large test chamber (13.84 m wide, 3.84 m high and 38 m long), the geometric scale of 1:12.5 results in quite higher Reynolds Number compared with similar studies in the literature.

The helicopter model, which has already been exploited in previous wind tunnel investigations (Refs. 16, 17), has four untwisted rectangular blades and a diameter of 0.75 m. A constant pitch angle of $10°$ was fixed in all tests, since the swashplate was not included in the current setup to trim the rotor. Forces and moments acting on the rotor have been measured for all points by implementing a six components balance nested inside the fuselage. The helicopter model was mounted on a series of traversing guides so that its relative position with respect to the ship could be changed. The SFS1 model was instrumented with several pressure taps connected to pressure scanners and high-frequency pressure transducers, in order to allow for both steady and unsteady pressure measurements. PIV of the ship airwake and of the helicopter inflow were carried out in order to have a better understanding of how the interacting flow fields affected the helicopter performance. Figure 2 shows the setup of the experiment mounted inside the GVPM.

Fig. 1. Closed-loop communication between flight simulator and wind tunnel.

Fig. 2. The test rig mounted inside the GVPM.

In order to simulate the landing trajectory, the rotorcraft was positioned in a series of points representative of a typical fore-aft landing trajectory and aerodynamic loads generated by the rotor were measured. The trajectory, as shown in Figure 3, consists of five points (P1 to P5) that can be divided into two distinctive segments: the initial phase in which the helicopter approaches the flight deck from stern side along the centerline of the flight deck and the descent phase, i.e. an oblique path towards landing spot, which is considered close to the center of the flight deck. Furthermore, three additional points above the landing point have been selected in order to simulate a vertical descent (P5 to P8). The reference frame shown in Figure 3 refers to the rotor reference frame whose x axis (X_r) is nose to tail, vertical axis is bottom to top (Z_r) and lateral axis is toward the advancing side of the rotor plane.

Fig. 4. Normalized vertical velocity measured by PIV above the longitudinal symmetry axis of the rotor (P5).
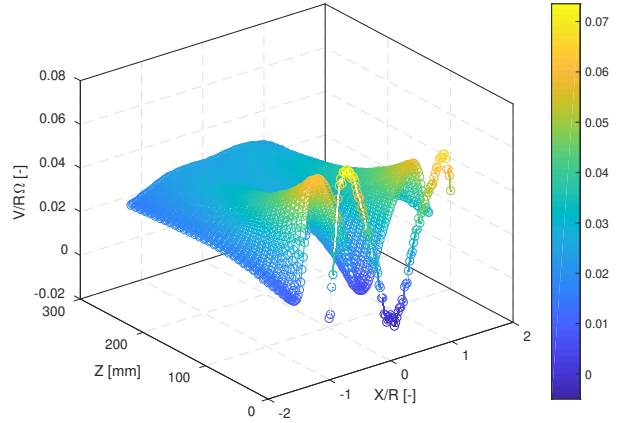

Fig. 3. Side-view of landing trajectory. Circles and crosses represent the centre of the rotor for that particular test condition.

The inflow of the rotor has been visualised using PIV technique which helps to study the correlation between loads and inflow parameters. To investigate the effect of wind velocity and direction, the experiment has been carried out in both windy and not windy conditions, for two different wind directions, i.e. headwind ($\beta = 0°$) and Red-30°($\beta = 30°$, port side). However, for the purpose of this paper only the database of headwind condition will be presented and analyzed. The chosen wind speed of 4.8 m/s corresponds to a full-scale velocity of 20 kt and to an advance ratio $\mu = U_\infty/V_{TIP} = 0.047$.

Figure 4 shows the profile of vertical velocity measured by PIV along the longitudinal axis of the rotor at different heights above the rotor plane, while the rotor is positioned in landing point (P5). Longitudinal axis and vertical velocity have been normalized with respect to radius and tip speed velocity, respectively, in order to be compared with simulation results in the following sections. It should be mentioned that the closest point of the PIV window was 4.8 cm above the rotor. So, the measurements are extrapolated in order to estimate the velocity just on top of the rotor disk.

Load measurements in headwind condition for both horizontal and vertical trajectories are presented in the last section in comparison with simulation results.

MULTIBODY MODELING

A multibody model of a 4-bladed rotor has been developed using MBDyn which is a free general purpose multibody dynamics analysis software (Ref. 18). MBDyn features the integrated multidisciplinary simulation of multibody systems, including nonlinear mechanics of rigid and flexible bodies subjected to kinematic constraints, along with smart materials, electric and hydraulic networks, active control and essential elements of rotorcraft aerodynamics (Ref. 19). The multibody model developed for this study consists of four rigid blades connected to the hub by implementing deformable hinges which generate the configuration dependent moments exchanged between two nodes. The hinges are considered to be very stiff in pitch and lead-lag degrees of freedom, however, the flapping stiffness has been set to allow a limited flapping deformation at the blade root. The flapping response of the blade in hover condition has been shown in Figure 5. Eigenanalysis of the rotor shows that non-dimensional flapping frequency is 35 percent higher than rotor frequency, $\nu_\beta = 1.35/rev$.
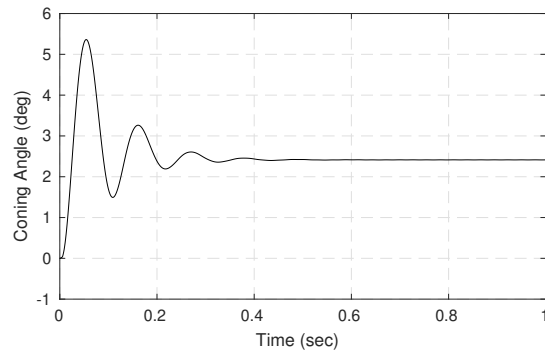
Fig. 5. Flapping response of the blade modeled in MBDyn-Hover condition.

The aerodynamic features of the blade has been modeled using NACA0012 as the airfoil, considering one percent of aerodynamic loss at blade tip. The geometry of the blade has been scaled up by geometric scale of 13 in order to have a model similar to Bo-105 which is the target of the new test campaign. The parameters of the experimental rotor and full scale model are summarized in Table 1.

It is worth mentioning that the ground effect has been incorporated into the simulation based on the model presented in Ref. 20. Fradenburgh conducted ground effect test using a two-bladed rotor with diameter of $D = 2ft$ operating at tip speed of approximately $600ft/s$. The results show that the thrust is increased by 15 percent when the rotor moves toward the ground from 3R to 1R. Similar results have been obtained in the test campaign performed at GVPM (Ref. 17).

As explained earlier, the current experiment dose not represent a dynamic maneuver, which means that the load measurements are related to the steady response of the rotor. So, at this stage, dynamic inflow is not implemented into the simulation environment and the induced velocity has been modeled using a linear distribution over the rotor disk (Ref. 12):

$$v_i = v_0(1 + \kappa_x r \cos\psi + \kappa_y r \sin\psi) \tag{3}$$

The classical vortex theory results give estimates of the factors κ_x and κ_y. Drees suggested following equations to approximate the linear variation of the inflow (Ref. 12):

$$\kappa_x = (f_x)(4/3)(1 - \cos\chi - 1.8\mu^2)/(\sin\chi) \tag{4}$$
$$\kappa_y = -2(f_y)\mu$$

f_x and f_y are empirical factors that are incorporated in each of the above equations to modify the inflow distribution in both lateral and longitudinal directions ($f_x = f_y = 1$ in Drees model). These factors have been set in order to generate same load coefficients, including thrust, torque and in-plane moments, while rotorcraft is positioned in the initial point of the landing trajectory (P1).

Figure 6 shows the comparison of the load coefficients from MBDyn and experiment for P1 in headwind condition, implementing the modified inflow with $f_x = 0.65$ and $f_y = 1$.

Table 1. Parameters of Wind Tunnel (WT) model and full scale model.

Characteristic	WT model	Full scale
Number of Blades	4	4
Rotor Radius(m)	0.375	4.9
Angular Velocity(rad/s)	270	44.4
Blade Chord(m)	0.032	0.27
Free Stream Velocity(m/s)	4.76	10.29
Advanced Ratio	0.047	0.047
Tip Mach Number	0.3	0.63
Tip Reynolds Number	$2.2e5$	$3.9e6$

This model has been used as the baseline model for further load analysis and development of the gust identification algorithm that will be explained in the following section.
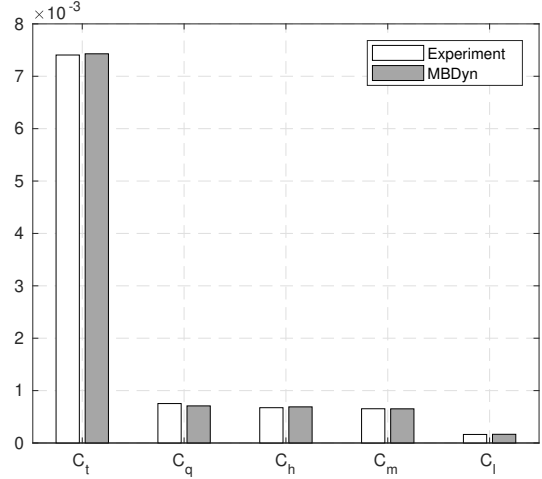
Fig. 6. Comparison of the rotor load coefficients from experiment and MBDyn for the initial point of the landing maneuver(P1).

INFLOW AND GUST IDENTIFICATION

Looking at the results of the load measurements while rotorcraft approaching the flight deck (Figure 7, 8), it can be seen that the velocity field above the rotor should be modified in order to get the same loads as the experiment for the whole landing trajectory. Considering the long term goal of this project, which has been explained in the introduction part, the velocity measurements cannot be implemented directly in the simulation environment. Consequently, an optimization algorithm has been developed in order to find the external gust component to reproduce the same loads. Further adjustment of the inflow empirical factors has been considered in order to slightly modify the contribution of lateral and longitudinal moments, if needed.

Gust velocity is considered to have a linear distribution in radial and azimuthal direction (similar to inflow), so it can be defined as the following equation:

$$V_g = V_{g_0} + V_{g_c} r \cos(\psi) + V_{g_s} r \sin(\psi) \tag{5}$$

Then, the optimization procedure has been done taking two steps as follows:

- finding a constant gust velocity V_{g_0} to match the thrust coefficient

So, following optimization problem is defined with V_{g_0} as the only optimization variable:

$$Min(J) \quad with \quad J = \sqrt{(C_t - C_{t_{wt}})^2} \tag{6}$$

It should be noted that since the ground effect has been implemented in the simulation, the variation of thrust is mainly caused by the altitude change. However, a small constant gust can be added to improve the matching.

- finding the first harmonics of gust velocity to generate same moment coefficients:

So, following optimization problem is defined with V_{g_c} and V_{g_s} as the optimization variables:

$$Min(J) \quad with \quad J = \sqrt{\left(\frac{C_m - C_{m_{wt}}}{C_{m_{wt}}}\right)^2 + \left(\frac{C_l - C_{l_{wt}}}{C_{l_{wt}}}\right)^2} \quad (7)$$

It should be mentioned that the velocity field above the rotor is considered as the combination of three different terms: free stream velocity, inflow of the rotor and external gust which is representative of the effects produced by the vortical flows generated by the ship. Clearly, inflow and gust velocities at each point above the rotor are functions of load coefficients, advance ratio and position (radial and azimuthal) of the point.

$$V_t = V_\infty + V_g(C_i, r, \psi, \mu) + v_i(C_i, r, \psi, \mu) \quad (8)$$

The simulation results implementing the solution of optimization algorithm as an external gust, are compared with the load measurements in headwind condition for all points along the landing and vertical trajectory.

Figure 7 compares the load coefficients for 5 points of the landing trajectory (P1 to P5). Horizontal axis refers to the same coordinate system shown in Figure 3. It should be noted that all the results are presented in rotor reference frame, as defined in Figure 3.

Regarding the experimental results, as it is expected, the thrust coefficient is increasing while rotorcraft approaching the landing point, since it enters the ground effect of the flight deck. The presence of the external wind also results in pitch and roll moments on the rotor. Due to the combination of the wind velocity and rotational velocity of the rotor, asymmetric thrust is generated in advancing and retreating side of the rotor plane, which produces a positive roll moment (roll to left). Considering the stiffness of the rotor, roll moment produces a positive pitch moment (nose up) by tilting the vector of the angular momentum in backward direction. This is also related to the distribution of the induced velocity in forward flight which results in reduced inflow in fore part and increased inflow in the aft part of the rotor (Ref. 21).

As it can be seen, the simulation results are highly consistent with the measurements which means the external gust is well representative of the environmental effects on rotor performance. There is an offset of 25% in torque coefficient that could be related to a higher profile drag of airfoil given the different Reynolds number and the additional drag of the inner part of the rotor in experiment compared with simulation in which there is no aerodynamic contribution for the hub.

Figure 8 refers to the same comparison for the vertical trajectory (P5 to P8). Here, horizontal axis refers to the rotor altitude from the flight deck as it has been shown in Figure 3. It is notable that in the landing point, which is 0.8R above the flight deck, the rotor is completely immersed in the ground effect and wake of the hangar wall. Similar to the previous
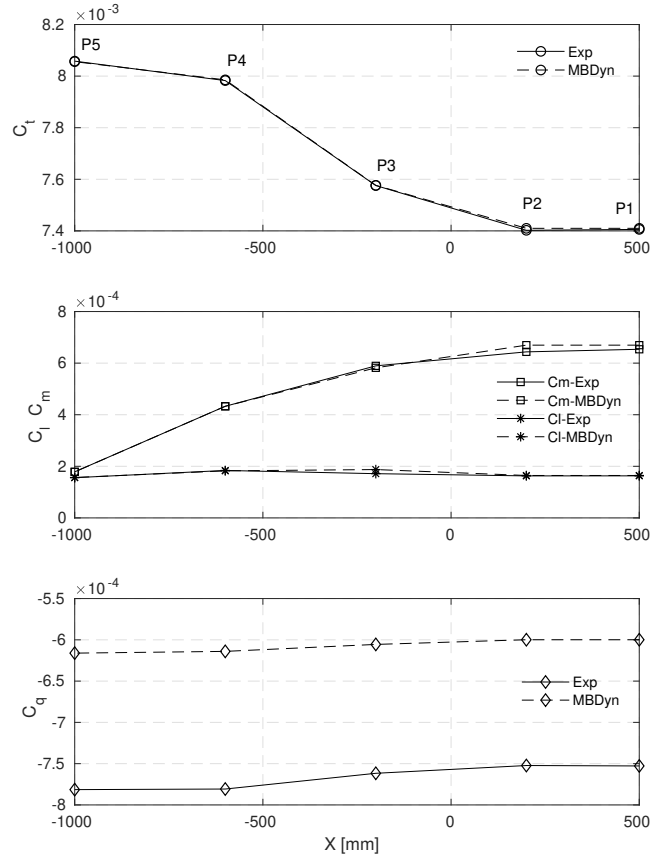

Fig. 7. Load coefficients along the horizontal landing trajectory-Comparison of wind tunnel measurements and MBDyn in headwind condition.

results, as the rotorcraft is going upward, thrust is decreasing and in plane moments are getting closer to the initial point of the landing in which the rotor is less affected by the ship airwake.

To be more clear, the first harmonics of the gust, normalized with respect to the tip velocity, are compared for all test points (Figure 9). The results show that initial points of the landing (P1 and P2) do not need additional modification of the velocity field. However, moving towards the landing point, the amplitude of the gust will be larger, which is consistent with the variation of the moment coefficients (Figures 7 and 8).

In order to assess the effect of external gust, the velocity field above the rotor has been shown without and with the presence of gust in Figure 10 and Figure 11, respectively. Both plots are related to the rotor positioned in landing point (P5). As it can be seen, the flow field has been modified to decrease the pitch moment (refer to Figure 7) by decreasing the velocity in rear part and increasing it in the fore part of the rotor. The roll moment generated due to pitch needs to be compensated in order to keep the net roll moment of the rotor almost unchanged (refer to Figure 7). Consequently, the gradient of velocity in lateral direction has been increased.

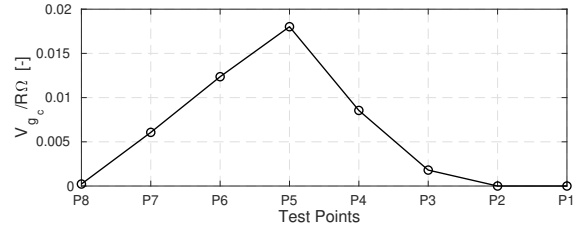Furthermore, the vertical velocity above the longitudinal sym-
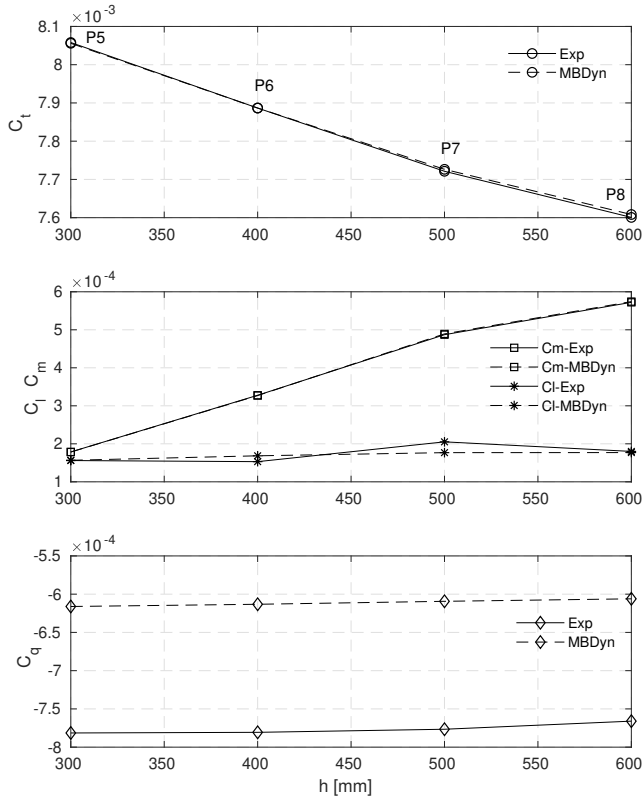
Fig. 8. Load coefficients along the vertical trajectory-Comparison of wind tunnel measurement and MBDyn in headwind condition.

Fig. 9. First harmonic of gust in different test points.

Fig. 10. Induced velocity distribution over the rotor disk area (P5).

metry axis of the rotor has been compared with PIV measurements. Since the inflow and gust implemented in the simulation have a linear distribution, a first order polynomial has been fitted to measurements to be compared with simulation. It should be mentioned that the inner part of the rotor which dose not generate aerodynamic lift has been removed with the same ratio used in the simulation. Figure 12 and Figure 13 refer to the landing point (P5) and P6 which has a vertical offset with respect to P5. It is clear in both figures that the external gust applied to the rotor is modifying the inflow by changing the gradient of velocity profile in order to generate the same moment coefficients.
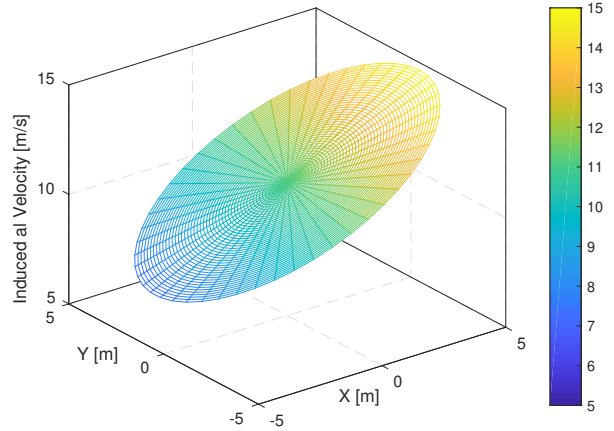
It is worth mentioning that the experimental blade and the simulated one cannot be identical in terms of aerodynamic efficiency, since they operate in two different Reynolds number. Furthermore, the aerodynamic characteristics of the experimental blade has been simplified by using NACA0012 airfoil in the multibody simulation environment. Consequently, it cannot be expected to generate same loads with identical velocities above the rotor, which is representative of the angle of attack of the blade.
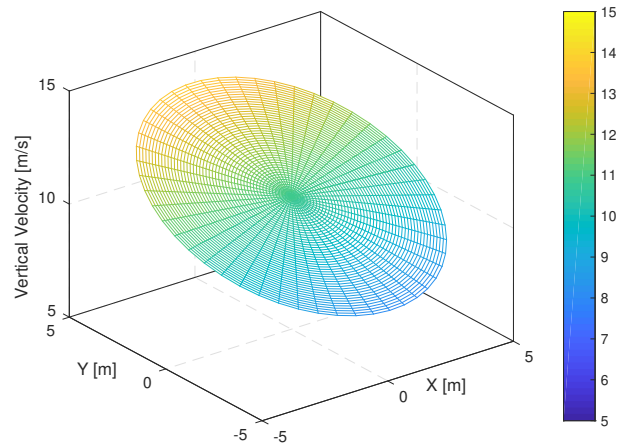
CONCLUSIONS

This work investigated the aerodynamic interaction between a scaled-down helicopter and simplified ship geometry in order

Fig. 11. Vertical velocity distribution over the rotor disk area (P5).

to develop a gust identification algorithm to be incorporated into the simulation environment to model the environmental effect on the rotor performance. To this aim, a series of wind tunnel experiment has been performed to simulate a typical fore-aft landing trajectory on the flight deck. The forces and moments generated by the rotor have been measured using a six components balance nested inside the fuselage. Also,
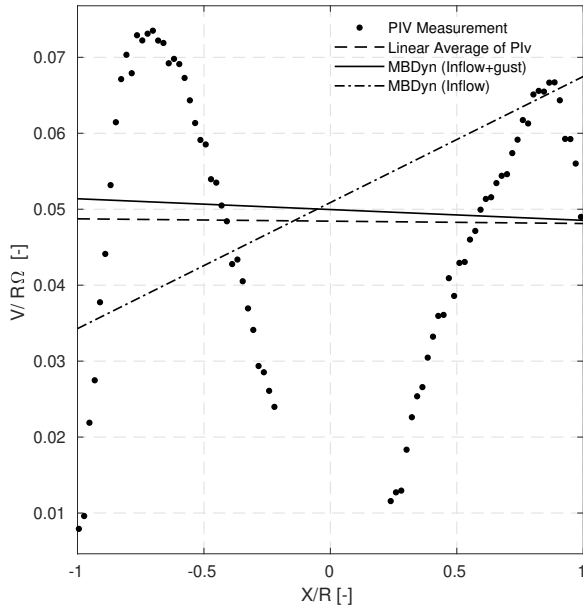
Fig. 12. Normalized vertical velocity along the longitudinal symmetry axis of the rotor-Comparison of wind tunnel measurement and MBDyn (P5).

Fig. 13. Normalized vertical velocity along the longitudinal symmetry axis of the rotor-Comparison of wind tunnel measurement and MBDyn (P6).

the in-plane velocity components above the longitudinal symmetry axis of the rotor have been visualized using PIV technique. A multibody model of the rotor has been developed in MBDyn for simulation purpose. A linear distribution of the inflow has been implemented, however, it has been modified with empirical factors in order to generate same load coefficients as the experiment at starting point of the landing maneuver. This model has been further modified by introducing a gust element into the model, while rotorcraft approaching the flight deck. The gust velocity is identified through an optimization algorithm with the objective of generating same in-plane moments as the experiment. Comparison of the results with experimental data shows that the gust element can modify the inflow of the rotor so that producing same loads in the presence of aerodynamic interaction. In the future, this approach will be implemented in a closed-loop communication between full-scale flight simulator and small-scale test setup in the wind tunnel.

Author contact:

Neda Taymourtash Neda.Taymourtash@polimi.it

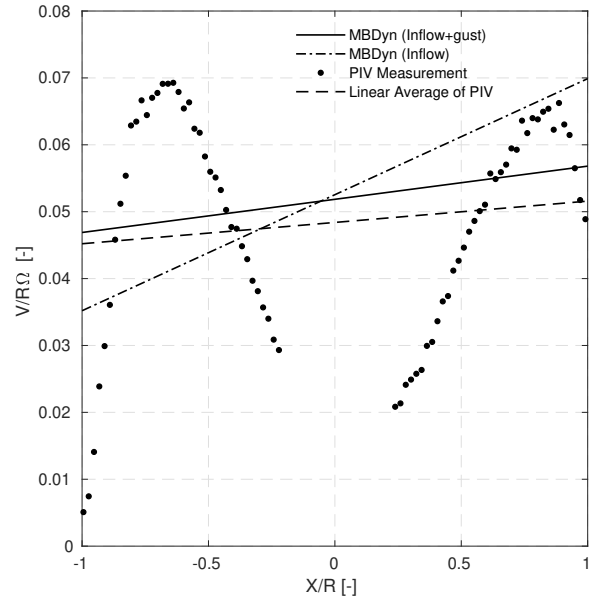Daniele Zagaglia Daniele.Zagaglia@polimi.it

Alex Zanotti Alex.Zanotti@polimi.it

Giuseppe Gibertini Giuseppe.Gibertini@polimi.it

Giuseppe Quaranta Giuseppe.Quaranta@polimi.it

REFERENCES

[1]Hodge, S. J., Zan, S. J., Roper, D. M., Padfield, G. D., and Owen, I., "Time-Accurate Ship Airwake and Unsteady Aerodynamic Loads Modeling for Maritime Helicopter Simulation," *Journal of american helicopter society*, Vol. 54, (2), April 2009, pp. 22005.

[2]Owen, I., White, M. D., Padfield, G. D., and Hodge, S. J., "A virtual engineering approach to the ship-helicopter dynamic interface a decade of modelling and simulation research at the University of Liverpool," *The Aeronautical Journal*, Vol. 121, (1246), December 2017, pp. 1833–1857.

[3]Quaranta, G., Barakos, G., White, M., Pavel, M., and Mulder, M., "NITROS: An Innovative Training Program to Enhance Rotorcraft Safety," American Helicopter Society International 74th Annual Forum, Phoenix, USA, May 2018.

[4]Kaaria, C. H., Forrest, J. S., Owen, I., and Padfield, G. D., "Simulated aerodynamic loading of an SH-60B helicopter in a ship's airwake," 35th European Rotorcraft Forum, Hamburg, Germany, September 2009.

[5]Chirico, G., Szubert, D., Vigevano, L., and Barakos, G. N., "Numerical modelling of the aerodynamic interference between helicopter and ground obstacles," *CEAS Aeronautical Journal*, Vol. 8, (4), December 2017, pp. 589–611.

[6]Bludau, J., Rauleder, J., Friedmann, L., and Hajek, M., "Real-Time Simulation of Dynamic Inflow Using Rotorcraft Flight Dynamics Coupled With a Lattice-Boltzmann Based Fluid Simulation," 55th AIAA Aerospace Sciences Meeting, AIAA SciTech Forum, Grapevine, Texas, January 2017.

[7]Oruc, I. and Horn, J. F., "Coupled Flight Dynamics and Computational Fluid Dynamics Simulations of Rotorcraft/Terrain Interactions," *Journal of Aircraft*, Vol. 54, (6), June 2017, pp. 2228–2241.

[8]Crozon, C., Steijl, R., and Barakos, G. N., "Coupled flight dynamics and CFD demonstration for helicopters in shipborne environment," *The Aeronautical Journal*, Vol. 122, (1247), January 2018, pp. 42–82.

[9]Pitt, D. M. and Peters, D. A., "Theoretical Prediction of dynamic inflow derivatives," 6th European Rotorcraft Forum, Bristol, England, September 1980.

[10]Peters, D. A., Boyd, D. D., and He, C. J., "FiniteState InducedFlow Model for Rotors in Hover and Forward Flight," *Journal of the American Helicopter Society*, Vol. 34, (4), October 1989, pp. 5–17.

[11]Peters, D. A. and He, C. J., "Correlation of Measured Induced Velocities with a Finite-State Wake Model," *Journal of the American Helicopter Society*, Vol. 36, (3), 1991, pp. 59–70.

[12]Johnson, W., *Rotorcraft Aeromechanics*, Cambridge University Press, first edition, 2013, Chapter 5, p. 136.

[13]He, C., Syal, M., Tischler, M. B., and Juhasz, O., "State-Space Inflow Model Identification from Viscous Vortex Particle Method for Advanced Rotorcraft Configurations," American Helicopter Society International 73rd Annual Forum, Texas, USA, May 2017.

[14]Reddy, K. R., Toffoletto, R., and Jones, K. R., "Numerical simulation of ship airwake," *Computers and fluids*, Vol. 29, (4), May 2000, pp. 451–465.

[15]Gibertini, G., Gasparini, L., and Zasso, A., "Aerodynamic design of a civil-aeronautical low speed large wind tunnel," AGARD 79th fluid dynamics panel symposium, Moscow, Russia, January 1996.

[16]Zagaglia, D., Zanotti, A., and Gibertini, G., "Analysis of the loads acting on the rotor of a helicopter model close to an obstacle in moderate windy condition," *Aerospace Science and Technology*, Vol. 78, 2018, pp. 580–592.

[17]Gibertini, G., Grassi, D., Parolini, C., Zagaglia, D., and Zanotti, A., "Experimental investigation on the aerodynamic interaction between a helicopter and ground obstacles," *Proceedings of the Institution of Mechanical Engineers, Part G: Journal of Aerospace Engineering*, Vol. 229, (8), 2015, pp. 1395–1406.

[18]Masarati, P., Morandini, M., and Mantegazza, P., "An efficient formulation for general-purpose multibody/multiphysics analysis," *ASME Journal of Computational Nonlinear Dynamics*, Vol. 9, (4), July 2014, pp. 041001–041001–9.

[19]Masarati, P., Piatak, D. J., Quaranta, G., Singleton, J. D., and Shen, J., "SoftInplane Tiltrotor Aeromechanics Investigation Using Two Comprehensive Multibody Solvers," *Journal of the American Helicopter Society*, Vol. 53, (2), 2008, pp. 179–192.

[20]Fradenburgh, E. A., "The helicopter and the ground effect machine," *Journal of the American Helicopter Society*, Vol. 5, (4), oct 1960, pp. 24–33.

[21]Elliott, J. W., Althoff, S. L., and Sailey, R. H., "Inflow measurement made with a laser velocimeter on a helicopter model in forward flight. Volume 1: Rectangular Planform Blades at an Advance Ration of 0.15," *NASA Technical Memorandum 100545*, 1985.